




Cite this: *Chem. Commun.*, 2023, 59, 3459

Received 25th January 2023,
Accepted 23rd February 2023

DOI: 10.1039/d3cc00350g

rsc.li/chemcomm

Surface modification of gold by carbazole dendrimers for improved carbon dioxide electroreduction†

Sota Yoshida,^a Masaki Sampei,^a Naoto Todoroki,^a *^{ab} Eri Hisamura,^c Kohei Nakao,^c Ken Albrecht ^{bc} and Toshimasa Wadayama^a

Four types of carbazole dendrimers were applied as modification molecules of Au surfaces to improve carbon dioxide electroreduction. The reduction properties depended on the molecular structures: the highest activity and selectivity to CO was achieved by 9-phenylcarbazole, probably caused by the charge transfer from the molecule to Au.

Practical carbon dioxide conversion processes are being considered to generate valuable chemicals for achieving carbon neutrality.¹ Electrochemical CO₂ reduction is crucial as one of the conversion processes of CO₂ to carbon monoxide (CO) and various chemicals such as hydrocarbons, alcohols, and formic acid, at ambient temperature and pressure. Therefore, practical electrolysis systems and the required materials have been intensively investigated.^{2–7} Previous research has shown that Au, Ag, and Zn electrodes selectively convert CO₂ to CO.⁸ In particular, Au showed relatively high efficiency for CO₂ reduction compared to that for hydrogen evolution, which is a competitive reaction of CO₂ reduction in aqueous solutions.^{8–10} However, the activity and selectivity of the Au electrode for converting CO₂ to CO remain insufficient for widespread application, and further research on CO₂ electrolysis systems is necessary to attain industrialisation.

We should notice that Au electrodes modified with various organic molecules enhance the reduction activity and selectivity to CO.^{11–19} For example, Zhao *et al.* used various amines to modify the surfaces of Au nanoparticles and found that oleylamine effectively improved the selectivity to CO.¹¹ Lee *et al.* investigated surface-modified Au nanoparticles experimentally

and theoretically using density functional theory calculations, where polymeric binders such as Nafion, polyvinyl alcohols, and polytetrafluoroethylene (PTFE) were used as modifying molecules. They showed that PTFE improved the selectivity to CO and the enhanced selectivity was originated from promoting CO₂ adsorption on the surface and suppressing the competing hydrogen evolution reaction (HER).²⁰ These reports clearly indicate that surface-modifying molecules affect the adsorption of CO₂ and H₂O on Au electrode surfaces and determine the efficiency of the electrochemical CO₂ reduction reaction (CO₂RR).

Dendrimers are dendritic polymers with precisely controlled structures that have potential applications as electronic and catalytic materials.^{21–23} Carbazole dendrimers (CDs), in particular, have unique photo- and electrochemical properties, and therefore are applicable as hole transport and luminescent materials.^{18,24} The molecular backbones, functional groups, and molecular weights of CDs can be easily controlled as a function of the generation (the number of repeated branching cycles). Furthermore, the chemical and physical properties of CDs can be tuned by the terminal and core functional groups. Due to molecular designability and resulting unique properties, CDs are also applicable for fundamental study to understand the relationship between the surface modifications of electrode surfaces.

In this study, four types of CDs were used to modify Au electrode surface for CO₂ electrochemical reduction. First, we showed that the conversion of CO₂ to CO using an Au disk electrode in an H-type electrochemical cell was enhanced most by the 9-phenylcarbazole (G1Ph) modification. Then, the enhanced electrochemical CO₂ reduction was also confirmed at high current density electrolysis using a gas diffusion electrode (GDE) cell designed for use in a practical CO₂ electrolyser.

A CD-modified polycrystalline Au disk ($\phi = 5$ mm) was used as the working electrode for CO₂ electrochemical reduction experiments in a CO₂-saturated 0.1 M KHCO₃ solution using an H-type electrochemical cell. The four CDs investigated are depicted in

^a Graduate School of Environmental Studies, Tohoku University, 6-2-2 Aramaki-aza-Aoba Aoba-ku, Sendai 980-8579, Japan. E-mail: naoto.todoroki.b1@tohoku.ac.jp

^b Japan Science and Technology Agency, PRESTO, Kawaguchi, Saitama 332-0012, Japan

^c Institute for Materials Chemistry and Engineering, Kyushu University, 6-1 Kasuga-koen, Kasuga-shi, Fukuoka 816-8580, Japan

† Electronic supplementary information (ESI) available. See DOI: <https://doi.org/10.1039/d3cc00350g>



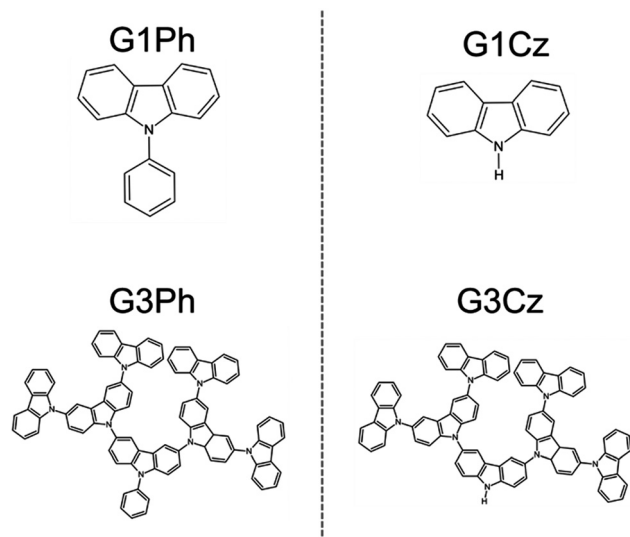


Fig. 1 Molecular structures of the carbazole dendrimers used for surface modification of the Au electrode.

Fig. 1. The CDs with phenyl (Ph) or NH groups are described as G x Ph (x = generation number of 1 and 3) and G x Cz, respectively. The surface modification by the CDs was conducted by drop-casting toluene solutions containing 0.1 mM CDs onto the Au disk electrode, followed by drying in air.

Fig. 2 shows the CO₂ reduction properties of the CD-modified and non-modified Au electrodes. In this condition, CO was the only product of the CO₂RR, irrespective of the kinds of CDs, and thus faradaic efficiencies and partial current densities for the generated CO are estimated (described in detail in supplementary information; ESI†). As shown in Fig. 2(a), the G1Ph-modified electrode showed enhanced faradaic efficiencies (FE_{CO}) relative to the non-modified electrode

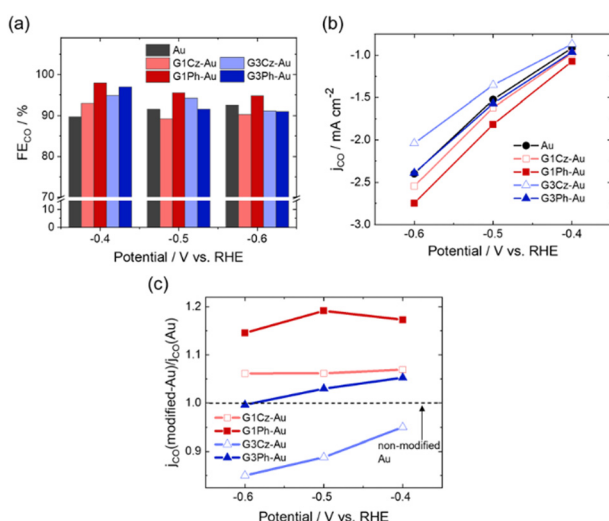


Fig. 2 (a) Faradaic efficiency and (b) partial current density for CO of surface-modified and non-modified Au electrodes evaluated in a CO₂-saturated 0.1 M KHCO₃ solution. (c) Normalized CO partial current density of G1Ph, G3Ph- and G1Cz, G3Cz-modified Au.

at -0.4 , -0.5 , and -0.6 V vs. reversible hydrogen electrode (RHE), particularly *ca.* 10% higher FE_{CO} at -0.4 V. In contrast, the G1Cz-, G3Cz-, and G3Ph-modified electrodes exhibited enhanced FE_{CO} at -0.4 V, while the efficiencies at -0.5 V and -0.6 V were almost identical to or lower than that of non-modified Au.

Fig. 2(b) and (c) show the partial current densities for CO (j_{CO}) of the CD-modified electrode surfaces, where the current densities are normalised to that of the non-modified Au electrode at each applied potential. As shown in (b), G1Ph- and G1Cz-modified Au electrodes exhibited enhanced j_{CO} , while the current densities of the G3Cz- and G3Ph-modified electrodes were comparable to and less than that of the non-modified electrode, respectively. These results suggest that CDs of smaller size (G1Ph and G1Cz) were favourable surface-modifying molecules. The maximum enhancement factor of j_{CO} was *ca.* 1.2 for G1Ph at -0.5 V, in comparison to non-modified Au (c). The results clearly indicate that introducing a phenyl group to the first generation carbazole (G1Ph) was the most effective surface modification at the applied potentials tested (-0.4 to -0.6 V).

Pb-underpotential deposition (UPD) was conducted for the CD-modified Au electrodes to estimate the active surface areas for the CO₂RR. Fig. 3(a) shows cyclic voltammograms recorded in an Ar-purged 1 mM Pb(OAc)₂ + 0.1 M NaOH solution for the

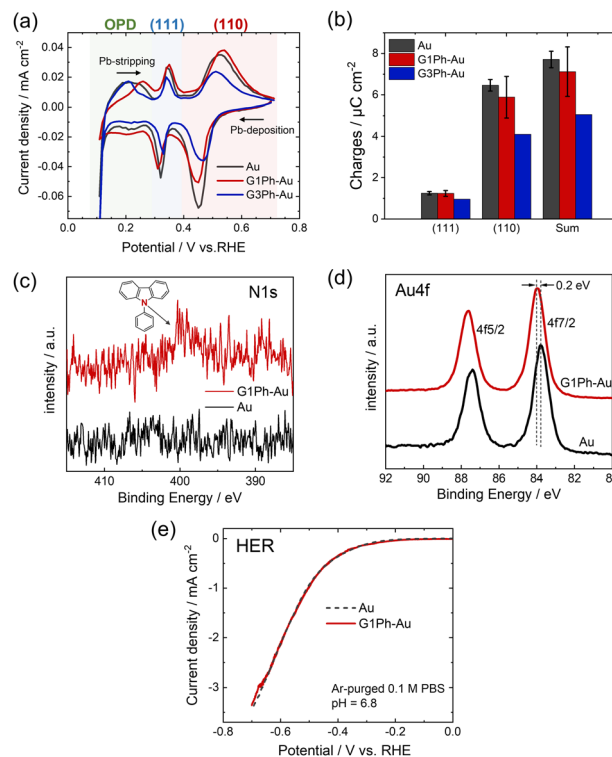


Fig. 3 (a) Cyclic voltammograms for Pb underpotential deposition collected in an Ar-purged 1 mM Pb(OAc)₂ + 0.1 M NaOH solution. (b) Pb-stripping charges estimated from (a). XP spectra of N 1s (c) and Au 4f (d) orbitals for G1Ph-modified and non-modified Au. (e) Linear-sweep voltammograms for the HER recorded in Ar-purged 0.1 M PBS electrolyte with a pH of 6.8.



most effective G1Ph-modified Au, less-effective G3Ph-modified, and non-modified Au electrodes. Because Pb-UPD potential is sensitive to the surface crystal facets of Au electrodes,²⁵ active surface areas of CD-modified Au electrode surfaces can be estimated for each crystal face of the modified Au electrodes. The potential region below 0.3 V vs. RHE (green) corresponds to the overpotential deposition (OPD) of Pb. The peaks located at the approximately 0.34 V (blue) and 0.51 V (red) regions in an anodic sweep can be ascribed to the stripping of Pb from the (111) and (110) facets, respectively, of the non-modified Au (black).²⁵ According to a previous report,²⁵ the Pb-stripping peak for the Au(100) face appears at *ca.* 0.4 V. In contrast, the corresponding peak is absent in Fig. 3(a), suggesting that the Au polycrystalline electrode used in this study was mainly composed of the (111) and (110) facets.

The Pb-stripping peaks for G1Ph- (red) and G3Ph-modified (blue) Au electrodes are located at similar potential regions for the non-modified one (black), suggesting that the (110) and (111) facets of the Au electrode surfaces are even active for CO₂ reduction sites under the presence of modifying molecules, though the estimated average Pb-stripping charges slightly decreased, particularly for the (110) facet, even by the effective G1Ph-surface-modification (Fig. 3(b)).

Furthermore, the Pb-stripping peaks shifted to approximately 20 mV higher potential for G1Ph-Au compared to the non-modified electrode. The positive potential shift suggests that G1Ph modification changed the electronic properties of the Au surface. Indeed, a similar shift has been reported for porphyrin-modified Au nanoparticles.²⁶ Modification with G3Ph caused a marked decrease in the corresponding charges, particularly in the (110) facet, suggesting that the lower efficiency might correspond to reaction-site blocking on the (110) facet.⁹ Therefore, the molecular-modification-dependent difference in Pb-stripping charge probably stems from differences in the molecular size of the CDs. The Pb-UPD experiment results suggest that G1Ph modification-enhanced CO₂ electrochemical reduction property is originated from suitable surface electronic states on the modified Au electrode, since the active surface area was nearly unchanged by the surface modification. In contrast, the G3Ph-modification decreased the surface active area, probably as a consequence of the larger molecular sizes of the CDs.

The change in the surface electronic state by G1Ph modification was also investigated by X-ray photoelectron spectroscopy (XPS). Fig. 3(c) and (d) show the XP spectra of the N 1s and Au 4f orbitals of the G1Ph-modified and non-modified Au. In the N 1s band of G1Ph-Au, the peak at 400 eV can be attributed to the C–N bond in the five-membered ring of carbazole.²⁷ Simultaneously, the Au 4f_{7/2} band of the G1Ph-Au shows a higher binding energy shift of *ca.* 0.2 eV, relative to that of non-modified Au. CDs have electron-donating properties,²⁸ and thus G1Ph may donate electrons to the Au electrode surface.

To understand the influence of CD surface modification on the competing HER, linear-sweep voltammetry (LSV) was conducted for G1Ph-modified Au in an Ar-purged 0.1 M phosphate-buffered saline solution with pH of 6.8, *i.e.*, water electrolysis at

the same pH (Fig. 3(e)). The LSV curves of G1Ph- (red) and non-modified (black dashed) Au electrodes are similar to each other, suggesting that the G1Ph modification does not affect the HER on the Au electrode surfaces. Zhang *et al.* proposed that the elementary step of CO₂ to a COOH* intermediate is the rate-limiting step for electrochemical CO₂ reduction on Au surfaces.² As shown previously for the Pb-UPD and XPS results (Fig. 3), the G1Ph-modification probably causes local electron enrichment at the Au electrode surface that can promote CO₂ reduction by reducing the activation energy for the first reductive step of CO₂ to COOH*.^{9,26}

Finally, we confirmed the enhanced CO₂ electrochemical reduction activity of the G1Ph-modified Au electrode at a high current density ($\sim 100 \text{ mA cm}^{-2}$). Fig. 4(a) presents a schematic of the flow-type GDE cell used in this study. The 100 nm-thick Au thin film deposited by magnetron sputtering (see ESI†) on a gas diffusion layer (Au-GDL) was used as a working electrode. Then, the Au-GDL was modified using a toluene solution of 0.1 mM G1Ph by the same procedure described for the Au disk electrode. Fig. 4(b) and (c) show the FE_{CO} and *j*_{CO} of the G1Ph- (red) and non-modified (black) Au-GDL. As clearly shown, the estimated FE_{CO} and *j*_{CO} increase *ca.* 10–20% by G1Ph modification, except for *j*_{CO} at -0.5 V , indicating the feasibility of the G1Ph-modified Au electrode for practical CO₂ electrochemical conversion to CO.

In conclusion, we investigated the electrochemical CO₂ reduction for CD-modified Au electrodes. The reduction property conducted by using Au disk electrodes and an H-type electrochemical cell depended on the backbone size (generation) and functional groups of the CDs. Among the CDs, G1Ph was most effective for CO₂ conversion to CO. Based on the results of XPS, Pb-UPD, and HER experiments, the enhanced electrochemical CO₂ reduction of the G1Ph-modified Au can be explained by a charge transfer from G1Ph to the Au surface. G1Ph-modification also enhanced high-current density electrolysis ($\sim 100 \text{ mA cm}^{-2}$) in a GDE electrochemical setup. These results show that the G1Ph surface modification of Au electrode

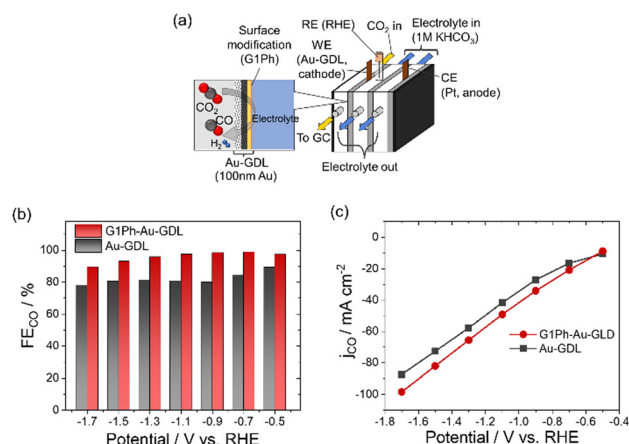


Fig. 4 (a) Schematic of the gas diffusion electrode type flow cell. (b) Faradaic efficiency and (c) partial current density for CO of G1Ph-modified and non-modified Au-GDL.



surfaces can facilitate a practical electrochemical conversion of CO₂ to CO.

This study was partly supported by JST, PRESTO Grand Number JPMJPR20T3 (N. T.) and JPMJPR18T2 (K. A.), Japan, and the Leading Initiative for Excellent Young Researchers from the Ministry of Education, Culture, Sport, Science & Technology of Japan (K. A.). The authors would also like to thank Dr. N. Akao and Dr. Y. Ohira for XPS measurements.

Conflicts of interest

There are no conflicts to declare.

Notes and references

- 1 S. Navarro-Jaén, M. Virginie, J. Bonin, M. Robert, R. Wojcieszak and A. Y. Khodakov, *Nat. Rev. Chem.*, 2021, **5**, 564–579.
- 2 B. Zhang, Y. Jiang, M. Gao, T. Ma, W. Sun and H. Pan, *Nano Energy*, 2021, **80**, 105504.
- 3 D. Higgins, C. Hahn, C. Xiang, T. F. Jaramillo and A. Z. Weber, *ACS Energy Lett.*, 2019, **4**, 317–324.
- 4 Y. Y. Birdja, E. Pérez-Gallent, M. C. Figueiredo, A. J. Göttele, F. Calle-Vallejo and M. T. M. Koper, *Nat. Energy*, 2019, **4**, 732–745.
- 5 N. Todoroki, N. Yokota, S. Nakahata, H. Nakamura and T. Wadayama, *Electrocatalysis*, 2016, **7**, 97–103.
- 6 K. Iwase, T. Kojima, N. Todoroki and I. Honma, *Chem. Commun.*, 2022, **58**, 4865–4868.
- 7 I. E. L. Stephens, K. Chan, A. Bagger, S. W. Boettcher, J. Bonin, E. Boutin, A. K. Buckley, R. Buonsanti, E. R. Cave, X. Chang, S. W. Chee, A. H. M. da Silva, P. de Luna, O. Einsle, B. Endrődi, M. Escudero-Escribano, J. V. Ferreira de Araujo, M. C. Figueiredo, C. Hahn, K. U. Hansen, S. Haussener, S. Hunegnaw, Z. Huo, Y. J. Hwang, C. Janáky, B. S. Jayatilake, F. Jiao, Z. P. Jovanov, P. Karimi, M. T. M. Koper, K. P. Kuhl, W. H. Lee, Z. Liang, X. Liu, S. Ma, M. Ma, H.-S. Oh, M. Robert, B. R. Cuenya, J. Rossmeisl, C. Roy, M. P. Ryan, E. H. Sargent, P. Sebastián-Pascual, B. Seger, L. Steier, P. Strasser, A. S. Varela, R. E. Vos, X. Wang, B. Xu, H. Yadegari and Y. Zhou, *JPhys Energy*, 2022, **4**, 042003.
- 8 Y. Hori, H. Wakebe, T. Tsukamoto and O. Koga, *Electrochim. Acta*, 1994, **39**, 1833–1839.
- 9 N. Todoroki, H. Tei, H. Tsurumaki, T. Miyakawa, T. Inoue and T. Wadayama, *ACS Catal.*, 2019, **9**, 1383–1388.
- 10 N. Todoroki, H. Tei, T. Miyakawa, H. Tsurumaki and T. Wadayama, *ChemElectroChem*, 2019, **6**, 3101–3107.
- 11 Y. Zhao, C. Wang, Y. Liu, D. R. MacFarlane and G. G. Wallace, *Adv. Energy Mater.*, 2018, **8**, 1801400.
- 12 J. Wang, J. Yu, M. Sun, L. Liao, Q. Zhang, L. Zhai, X. Zhou, L. Li, G. Wang, F. Meng, D. Shen, Z. Li, H. Bao, Y. Wang, J. Zhou, Y. Chen, W. Niu, B. Huang, L. Gu, C. S. Lee and Z. Fan, *Small*, 2022, **18**, e2106766.
- 13 Q. Lenne, Y. R. Leroux and C. Lagrost, *ChemElectroChem*, 2020, **7**, 2345–2363.
- 14 J. Wang, F. Xu, Z. Y. Wang, S. Q. Zang and T. C. W. Mak, *Angew. Chem., Int. Ed.*, 2022, **61**, e202207492.
- 15 M. Tan, X. Han, S. Ru, C. Zhang, Z. Ji, Z. Shi, G. Qiao, Y. Wang, R. Cui, Q. Luo, J. Jiao, Y. Li and T. Lu, *Nano Res.*, 2023, **16**, 2059–2064.
- 16 T.-H. Wang, C.-Y. Lin, Y.-C. Huang and C.-Y. Li, *Electrochim. Acta*, 2023, **437**, 141500.
- 17 Y. Shi, M. Hou, J. Li, L. Li and Z. Zhang, *Acta Phys.-Chim. Sin.*, 2022, **38**, 2206020.
- 18 M. Hou, Y. X. Shi, J. J. Li, Z. Gao and Z. Zhang, *Chem. – Asian J.*, 2022, **17**, e202200624.
- 19 D.-H. Nam, P. De Luna, A. Rosas-Hernández, A. Thevenon, F. Li, T. Agapie, J. C. Peters, O. Shekhah, M. Eddaoudi and E. H. Sargent, *Nat. Mat.*, 2020, **19**, 266–276.
- 20 J. H. Lee, S. Kattel, Z. Xie, B. M. Tackett, J. Wang, C.-J. Liu and J. G. Chen, *Adv. Funct. Mater.*, 2018, **28**, 1804762.
- 21 K. Albrecht, K. Matsuoka, K. Fujita and K. Yamamoto, *Angew. Chem., Int. Ed.*, 2015, **54**, 5677–5682.
- 22 K. Albrecht and K. Yamamoto, *J. Am. Chem. Soc.*, 2009, **131**, 2244–2251.
- 23 N. D. McClenaghan, R. Passalacqua, F. Loiseau, S. Campagna, B. Verheyde, A. Hameurlaine and W. Dehaen, *J. Am. Chem. Soc.*, 2003, **125**, 5356–5365.
- 24 D. Astruc, E. Boisselier and C. Ornelas, *Chem. Rev.*, 2010, **110**, 1857–1959.
- 25 N. Mayet, K. Servat, K. B. Kokoh and T. W. Napporn, *Surfaces*, 2019, **2**, 257–276.
- 26 Z. Cao, S. B. Zacate, X. Sun, J. Liu, E. M. Hale, W. P. Carson, S. B. Tyndall, J. Xu, X. Liu, X. Liu, C. Song, J.-h. Luo, M.-J. Cheng, X. Wen and W. Liu, *Angew. Chem., Int. Ed.*, 2018, **57**, 12675–12679.
- 27 M. Ayiania, M. Smith, A. J. R. Hensley, L. Scudiero, J.-S. McEwen and M. Garcia-Perez, *Carbon*, 2020, **162**, 528–544.
- 28 P. Ledwon, *Org. Electron.*, 2019, **75**, 105422.

